D31

3.6A INTERFEROMETER APPLICATIONS OF VHF RADARS*

J. Rottger**

EISCAT Scientific Association
Box 705
S-98127 Kiruna, Sweden

INTRODUCTION

Using a spaced antenna setup of a VHF radar, the spatial distribution of amplitudes and phases of the radar echoes from the troposphere, stratosphere and mesosphere can be measured. Combining in a suitable analysis procedure the complex digital samples from the different receiving antennas is consistent with the radar interferometer method. In addition to the well-known parameters measured with the commonly applied Doppler and drifts methods, i.e., reflectivity and mean and fluctuating velocity, the interferometer technique allows to measure the angular spectrum of the returns. It gives supplementary useful information on wave and turbulence structures and on the baroclinicity of the detected structures as well as improves the accuracy of the vertical velocity measurements.

This technique, which was first applied with the spaced antenna system of the SOUSY-VHF-Radar in W. Germany, as well as some first examples of results are described here. These comprise the measurements of the horizontal and vertical velocities of the mean flow as well as of turbulence structures, the aspect sensitivity and the tilt of layers from which the baroclinicity can be estimated. Particularly, results of interferometer measurements of the vertical and horizontal phase velocities and wavelengths of gravity waves in the stratosphere are displayed. The latter results are also discussed in terms of the generation and propagation of these waves.

RADAR INTERFEROMETRY

The interferometer technique is most extensively used in radio astronomy (e.g., KRAUS, 1966). It is also applied in the radar technique (e.g., WOHLLEBEN and MATTES, 1973). Under special conditions it was also employed in radar investigations of the ionosphere (e.g., PFISTER, 1971; FARLEY et al., 1981; WHITEHEAD et al., 1983), although only Farley et al. used the name "radar interferometry". First attempts to apply it to VHF radar investigations of the lower and middle atmosphere were reported by ROTTGER and VINCENT (1978), VINCENT and ROTTGER (1980), ROTTGER (1983) and ROYRVIK (1983). The commonly utilized methods in the MST/VHF radar operations are the Doppler (beam swinging) method and the spaced antenna (drifts) method. Although in both methods the amplitudes and phases of the signals are recorded (coherent detection), an evaluation of the spatial variations of the phases of the radar echoes (radar interferometry) is not accomplished.

The Doppler method uses different preset beam directions (obtained either by appropriate positioning of a dish antenna or by fixed instrumentally implemented phasing between submodules of a phased-array antenna system). Combining the radial Doppler velocities measured at different beam directions yields the

---

* To be published also in: Preprint Volume, American Meteorological Society, 22 Conference on Radar Meteorology, Zurich, Switzerland, 1984.

**Presently at Arecibo Observatory, Arecibo, Puerto Rico, on leave from Max-Planck-Institut fur Aeronomie, Lindau, W. Germany.

total bulk velocity vector of the moving scatterers. If one does receive the radar signal with two different (spatially separated) antenna systems as shown in Figure 1, and inserts a suitable phase shift $\Delta\phi$ to the recorded data one can point the receiving antenna beams to different positions without changing the hardware (insertion of phase differences before taking the data). This kind of interferometer method we may call "postset beam direction". Whereas the method of "preset beam direction" (i.e., the commonly applied Doppler method) uses mostly the same fixed beam direction for transmission and reception and therefore does not allow a change of beam direction after the data were recorded, the method of "postset beam direction" has to use a fixed transmitter beam with beam width broader than the steering angles of the receiver beams. However, the (receiver) beam direction of the latter method can still be varied (within the limit of the transmitter beam width) after the data are recorded on tape. It has to be noted here that both these methods work for reflection from small or extended targets as well as for volume scattering. Because the beam widths of the transmitter and receiver antennas are equal in the preset beam direction method, it yields a better signal-to-noise ratio than the postset beam direction method where part of the transmitter energy is lost because the receiver antenna beam picks out only a portion of the wide transmitter antenna beam. However, the postset method has other advantages since it allows to scan (simultaneously) the total area illuminated by the transmitter beam and thus yields improved information (high spatial and temporal resolution) on the atmospheric structure detected by the radar. The example in Figure 1 indicates a wave-like structure overhead the radar antennas, which can be scanned not only at the indicated positions, but (provided the receiver antennas are suitably configurated) also at positions in between, yielding the radial velocities and reflectivities as a function of incidence angle (angular spectrum).

The configuration of the radar interferometer array can be computed in a way similar to the standard procedure of antenna theory. Assume that N individual antenna elements with equal spacing d are horizontally lined up to form a multi-element array. In the array far-field $r>(Nd)^2/\lambda$, where λ is the radar wavelength, the antenna polar diagram is

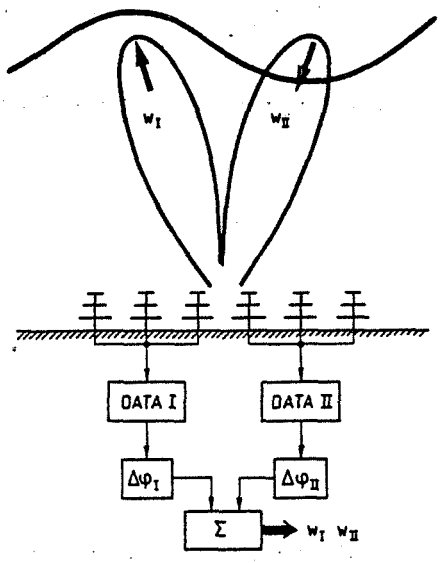

Figure 1. Principle of postset beam steering.

$$E(\delta) = \sum_{n=1}^{N} E_n(\delta)\exp(i(2\pi d\sin\delta(n-1)/\lambda + \Delta\phi_n)), \quad (1)$$

where $E_n(\delta)$ is the pattern of an individual element, δ is the zenith angle and $\Delta\phi_n$ is the relative phase placed on this element. Since $E_n(\delta)$ does not vary considerably in our applications (small δ), we assume $E_n(\delta) = E_n$ = const, and $\phi_n(\delta) = 2\pi d\sin\delta(n-1)/\lambda$. Equation (1) can be written as

$$E(\delta) = \sum_n E_n \exp\,(i(\phi_n(\delta) + \Delta\phi_n)) \quad . \quad (2)$$

The integral of (2) over δ is proportional to the complex signal C_n which is measured at the antenna n. For $\Delta\phi_n = 0°$ and $d < \lambda$ the antenna system has a main lobe at $\delta = 0°$ (zenith) with width $\delta_B = \arcsin(\lambda/Nd)$. The direction of the main lobe δ_o can be changed by applying a linearly progressing phase $\Delta\phi_n$ from element to element:

$$\Delta\phi_n = 2\pi d\sin\delta_o(n-1)/\lambda\,. \quad (3)$$

Note, that in the radar inferometer application $\Delta\phi_n$ is inserted during the data processing procedure. Also grating (side) lobes occur in this application for $d > \lambda$, which have to be suitably suppressed.

Whereas this method of beam steering works principally for hard targets (reflecting structures) and for soft targets (scattering structures) it can in a basically similar way also be used to measure the incidence or zenith angle of reflecting discrete structures or small blobs or patches of turbulence irregularities and to correct velocity estimates. This is briefly sketched in Figure 2.

Let us assume that diffuse reflection takes place from a rough surface or structure S which is slightly tilted to the horizontal by an angle δ'. This structure shall move with a velocity given by the horizontal component U and the vertical component W. A radar with vertically pointing transmitting antenna A_o with beam width larger than δ' measures the radial velocity

$$V' = W^*-U^* = W\cos\delta'-U\sin\delta'. \quad (4)$$

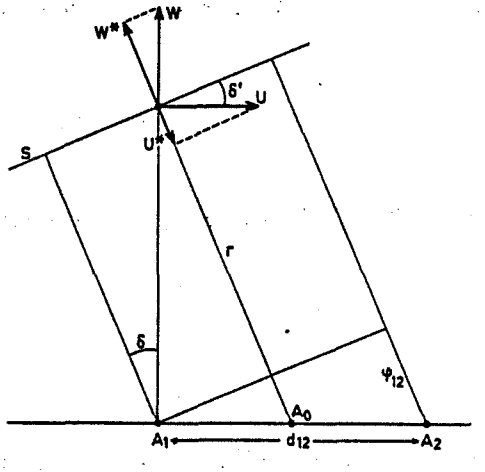

Figure 2. Principle of measuring incidence angle δ.

Thus, even when knowing (i.e., measuring by other means) the horizontal velocity U, the vertical velocity is still incorrectly measured, if δ' is unknown (ROTTGER, 1981).

When we apply the interferometer technique with n=2 antennas A_1 and A_2, we can compute the complex cross correlation function of the signals measured at A_1 and A_2. Its phase at zero lag (τ=0) is $\Delta\phi_{12}$, which yields the tilt or incidence angle

$$\delta' = \arcsin (\Delta\phi_{12}\lambda/2\pi d_{12}). \quad (5)$$

Measuring the horizontal velocity U with the spaced antenna drifts method and the radial velocity V' from the time derivative of the correlation function near zero

$$V' = d\phi/d\tau \; \lambda/4\pi, \quad (6)$$

we obtain the corrected vertical velocity

$$W = (V'+U\sin\delta)/\cos\delta. \quad (7)$$

This method (ROTTGER, 1984) can be refined by applying a complex cross spectrum analysis (FARLEY et al., 1981), which allows to improve the signal-to-noise ratio and to discriminate (by means of Doppler sorting) between separate discrete scatterers or reflectors in the beam which move with different velocities.

This radar interferometer method allows not only the measurements of the horizontal wind component (when pointing the receiver beams as done in the preset beam direction Doppler method) but also the tilt or inclination (baroclinicity) and the aspect sensitivity of reflecting structures. It is also suitable for gravity wave investigations as described in a later section, as well as will allow to measure the momentum flux, i.e., the cross product between U and W as done by VINCENT and REID (1983) with preset beam directions.

EXPERIMENT AND DATA ANALYSIS

The interferometer investigations were done by analysing a data set taken in an earlier experiment carried out from 3-14 September 1980 with the SOUSY-VHF-Radar. The radar was operated at 53.5 MHz with 500 kW pulse peak power and 4% duty cycle. Since this experiment concentrated on the stratosphere and mesosphere, an 8-bit complementary code with 10-µs bit length was used, providing a range resolution of 1.5 km at the maximum average power 20 kW. The lowest recorded height was 13.5 km and the spaced antenna method was applied using the 196 Yagi system for transmission and the 3x32 Yagi system for reception (Figure 3). The data were coherently preintegrated over 1/6 s, yielding an effective sampling rate of 1/2 s for the 3 spaced antennas. Since the earlier data analysis (ROTTGER, 1981) showed a fairly pronounced wave activity in the stratosphere, the interferometer analysis was applied to a part of this data set in order to test the applicability of the method and to gain a more profound insight into the gravity wave phenomena.

We first had to compute the optimum interferometer antenna pattern E, resulting from the combination of the spaced antenna setup E_R, the transmitter antenna pattern E_T and the aspect sensitivity A. This was done by just combining two spaced antenna modules (3-1, 3-2 or 2-1) at a time which is equivalent to a two-element interferometer with quasi-continuous aperture distribution. It allows to steer the interferometer beam in an E-W direction, 26° E of N and 26° W of N. Taking into account the positions of single Yagis of the spaced antenna system (fed with equal phase for each module), equation (1)

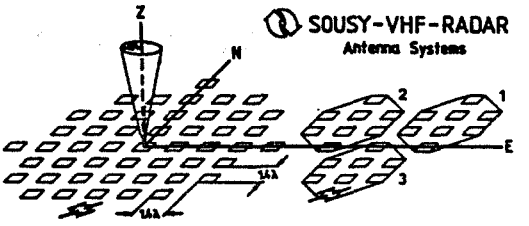

Figure 3. Antenna system with main antenna (3155 m^2 area) and three spaced antenna modules (3x395 m^2 area) pointing vertical. Distance between centres of spaced antennas was 24 m (2-1) and 28 m (3-1,3-2).

was used with n=2 to calculate E_R. The aspect sensitivity was assumed as A=2 dB/degree. The total interferometer pattern then becomes:

$$E = E_R \cdot E_T \cdot A.$$

By varying the phase difference $\Delta\phi$ between two modules, the maximum difference between the two interferometer lobes closest to the zenith was searched for. The optimum suppression of this simple 2-element interferometer configuration was found to be 6 dB. Integrating the antenna pattern over δ from -6° to +6° yields an apparent interferometer beam direction $\bar{\delta}$=1.2° for the combinations 3-2 and 3-1. The corresponding $\Delta\phi$ then was used to transform the complex data recorded with antenna 3, 2 and 1, which are available on tape. After complex summation (Figure 1 and equation (1)), the procedure was applied to calculate the first moment of the Doppler spectrum, respectively the radial velocity W*, which in the following treatments is reasonably assumed to be equal to W.

OBSERVATIONS

In Figure 6 of ROTTGER (1981) a series of quasi-vertical velocity data is shown which was obtained measuring with one antenna. The observed velocity oscillations at periods of 4-6 minutes are clearly repeated in Figure 5 of this paper. These results were obtained by combining the data of antenna 3 and 1 after introducing phase shifts $\mp\Delta\phi$. As described in the preceding section this corresponds to tilting the interferometer beam ±1.2° off the vertical direction. The average horizontal probing distance at these tilt angles is about 800 m at 20 km altitude. It is clearly seen that this tilting results in a phase shift of the wave-like oscillations in Figure 5. The curves with open circles correspond to a tilt in direction 3-1 (about N) and the closed circles in direction 1-3 (about S). The phase delay of the wave structure was not so pronounced when observing with antennas 3-2/2-3, and it was not observed with 2-1/1-2. We, thus, conclude that we observed a wave propagating into the direction around 26° E of N.

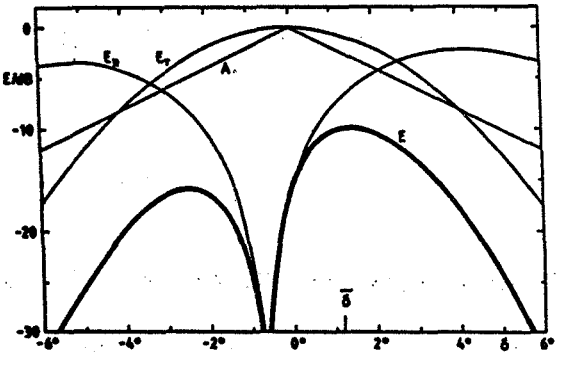

Figure 4. Optimum interferometer pattern E, resulting from pattern of transmitter antenna E_T, spaced antenna E_R and aspect sensitivity A.

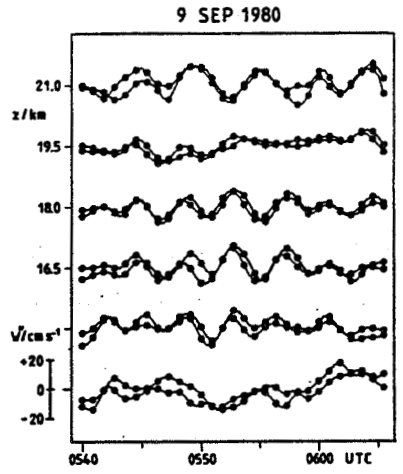

Figure 5. Radial velocity time series, measured with interferometer beam tilted to zenith angles 1.2° N (open circles) and 1.2° S (closed circles) for range gates at altitudes z.

These observations can be improved by a more quantitative approach which results in the data displayed in Figure 6. Here we have shown the average phase difference between the oscillations of the radial quasi-vertical velocity observed with different beam directions. The notations N32, S32, N31, S31 indicate the directions (N or S) to which the antenna combinations 3-2 and 3-1 were tilted. The phase angle ϕ_w was calculated by a cross spectrum analysis of the quasi-vertical velocity time series over a time interval of 90 min from 0446-0616 UT. The cross spectrum analysis yields also the coherence of two time series. Since the observed oscillations are not monochromatic but cover a band corresponding to about 4-6 min period (ROTTGER, 1981), the average phase difference ϕ_w was calculated by a weighted average using the coherence as a weighting function. This procedure suppressed noisy velocity fluctuations and filtered out the period band of about 4-6 min.

It is evident from Figure 6 that the phase difference ϕ_w changes its sign when steering the interferometer from the northward to the southward tilt. The absolute phase difference was in the range of about 5°-15°. There are obviously some fluctuations superimposed on these estimates of ϕ_w. These are partly because of the nonstationary wave oscillations, their nonmonochromatic nature and also due to the fact that the interferometer sidelobe (positioned at about opposite zenith direction of the main lobe, Figure 4) is suppressed by only 6 dB. This obviously yields spurious contributions from the opposite direction. It is also likely that the reflectivity structures are slightly

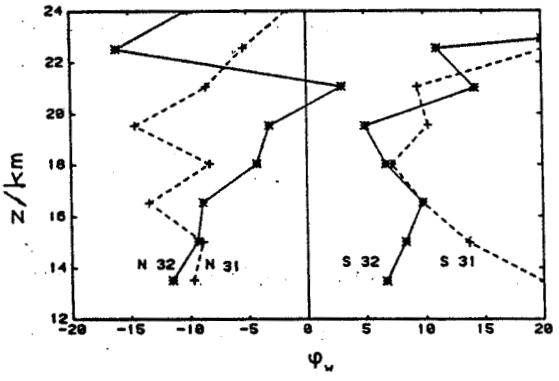

Figure 6. Phase difference ϕ_w of radial velocity oscillation, measured with beams tilted to N and S.

tilted with respect to the horizontal (due to the wave modulation), which results in a change of incidence angle (and aspect sensitivity model in Figure 4) and consequently of the measured radial velocity. Principally, however, the results of Figure 6 prove that the applied interferometer method is consistent with the expectations.

Not only fluctuating or oscillating radial velocities can be evaluated with this method but also the average vertical and horizontal velocity. We have briefly outlined the deduction of the average vertical velocity in a previous section and it was discussed also by ROTTGER (1981), and we will describe here the approach to measure the horizontal velocity with the interferometer setup. Even at small off-zenith angles, the component of the horizontal velocity is not negligible and can be measured. When averaging over 90 min with the interferometer beam at the same positions N32,... as described earlier, we measure the mean radial velocity $\overline{V}'$ (Figure 7). It is again noticed that also $\overline{V}'$ has a different sign with the beam towards N and S. If the method is correct, the difference $\Delta=\overline{V}'(N)-\overline{V}'(S)=0$. The single stars and crosses in Figure 7 indicate Δ for the antenna configurations 3-2 (*) and 3-1 (+). The residual Δ of less than 0.1 ms^{-1} is acceptably smaller than $\overline{V}'$.

The average U_R obtained with 3 antenna combinations can be transverted into the horizontal velocity vector because we know the tilt angle δ. This yields the average wind speed U_o and direction α_o (Figure 8). The subscript i denotes the values deduced with the described interferometer technique and the subscript D the values deduced with the spaced antenna drift method (ROTTGER, 1981). The similarity of these radar results with radiosonde data (⊠) gains a very reliable confidence that the interferometer method is applicable and practical.

WAVES AND TURBULENCE

Combining the results of the cross spectrum analysis of the wave events shown in Figure 5, the horizontal wave vector, respectively, horizontal phase speed V_p, wavelength λ_h and propagation direction α_p can be estimated. The analysis also yields the mean amplitude of the vertical velocity W and the mean period T of the wave. Results are shown in Figure 9. In this diagram additionally the horizontal width b of the volume probed with the applied beam

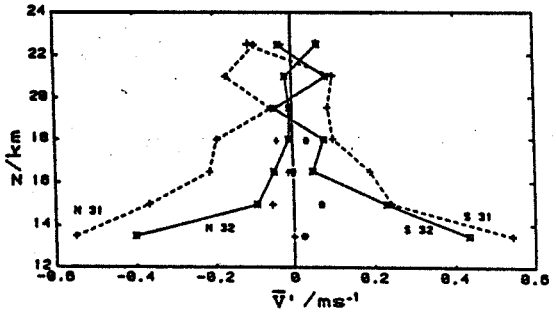

Figure 7. Average radial velocity $\overline{V}'$, measured with beams tilted to N and S.

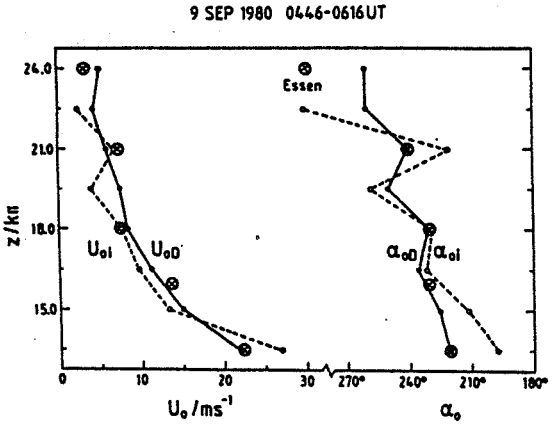

Figure 8. Average wind speed U_o and direction α_o measured with interferometer (I) and spaced-antenna drifts (D) compared with radiosonde data from Essen (⊠).

widths is indicated. It is much smaller than the horizontal wavelength λ_h. The vertical wavelength λ_z of the gravity wave events is found by cross spectrum analysis of adjacent altitude gates. Since we observed coherent wave events only over a few kilometers height range (ROTTGER, 1981) and the phase differences with height are not too pronounced, the measurement of the vertical wavelength is not too consistent. The vertical wavelength and mean period change with altitude which also makes the determination of λ_z difficult.

Knowing the horizontal wave vector from the described measurements, one can find the horizontal phase velocity V_p (with respect to the fixed observer) and the propagation direction α_p of the wave event. These are shown in Figure 10, where additionally the average background wind speed U_o and its direction α_o are inserted. We can summarize the results of the analysis of these wave events observed in the lower stratosphere:

(1) The horizontal wavelengths are about 10-20 km and increasing with height,
(2) The vertical wavelengths are 2-3 times larger than the horizontal wavelengths,
(3) The wave periods increase with altitude from about 250 s to 300 s,
(4) The mean vertical velocity amplitude increases with height from about 8 cm s^{-1} to 10 cm s^{-1},
(5) The direction of wave propagation is almost constant with altitude,
(6) The phase speed of waves is about 40 ms^{-1} and constant with altitude, it is several times larger than the mean wind above 15 km altitude,
(7) The phase speed and direction are similar to wind speed and direction close to the lowest height observed (~13.5 km),
(8) The wave phases propagate downward,
(9) From (7) and (8) it is deduced that these waves are probably generated in wind shear regions close to 13.5 km altitude.

Average vertical velocities connected with synoptic scale disturbances were analysed by ROTTGER (1981). It was estimated that they are some 10 cm s^{-1} in the lower stratosphere and can be determined with an accuracy of about 20% if one does not correct for possible tilts. Qualitative analyses of baroclinicity in the troposphere indicated tilt angle changes during frontal passages, but quantitative investigations are still under way. The aspect sensitivity (angular spectrum) and tilt (incidence) angles were also measured by VINCENT and ROTTGER (1980).

Incidence angle variations can be either explained by varying tilt angles of extended reflecting structures or by turbulence blobs moving through the

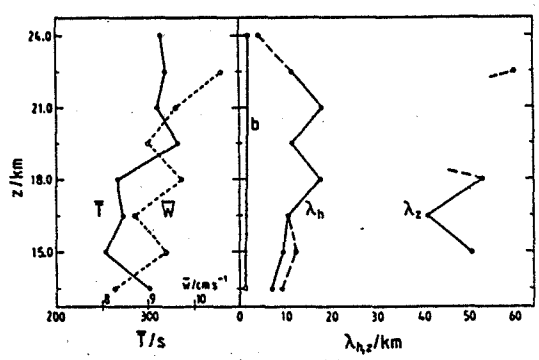

Figure 9. Height profiles of average period $\bar{T}$, quasi-vertical velocity $\bar{W}$, horizontal (λ_h) and vertical (λ_z) wavelengths.

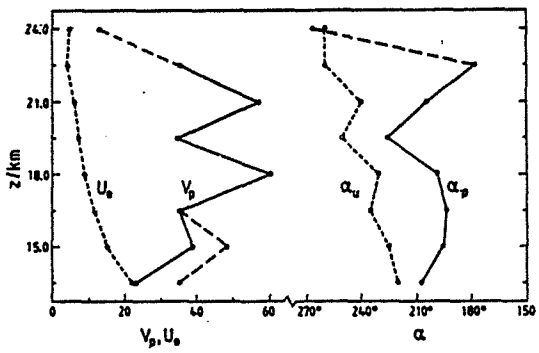

Figure 10. Phase speed V_p and propagation direction α_p of waves, and mean wind speed U_o and direction α_o.

antenna beam. The latter case may occur in the mesosphere as suggested by ROTTGER et al. (1979). To test this hypothesis we have analysed a similar event which is displayed in the height-time-intensity plot of Figure 11. It shows a fairly thin and short-lived structure at about 65 km altitude after 0710 UT. Analysing this event with the cross spectrum interferometer technique yielded the results displayed in Figure 12 (see IERKIC and ROTTGER (1984) for details). Here P_1, P_2 and P_3 are the power spectra measured over 40 s at the three different spaced antennas. They clearly show a change of Doppler shift from positive values at the beginning to negative values at the end of the event. In the lower diagrams the coherence C_{13} and phases ϕ_{13} of signals measured at antennas 1 and 3 are displayed. It is evident that the phases changed as a function of time, which would not be expected if the scattering target would have remained overhead and moved down and up in the radar beam, according to the Doppler shift. The only explanation of these observations is that a small scattering blob was in the antenna beam, moving with vertical and horizontal velocity. This analysis evidently proves the great advantage in applying the interferometer technique to avoid misinterpreting the velocity measurements, by assuming only a vertical velocity component inferred from the Doppler spectra.

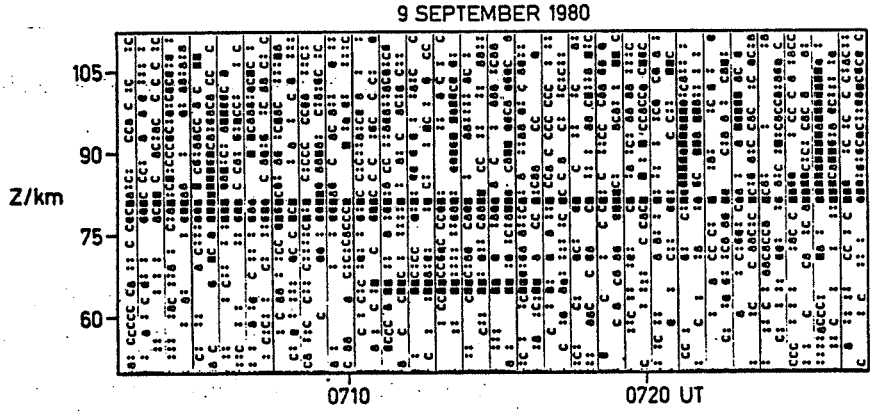

Figure 11. Height-time-intensity plot of mesospheric signals.

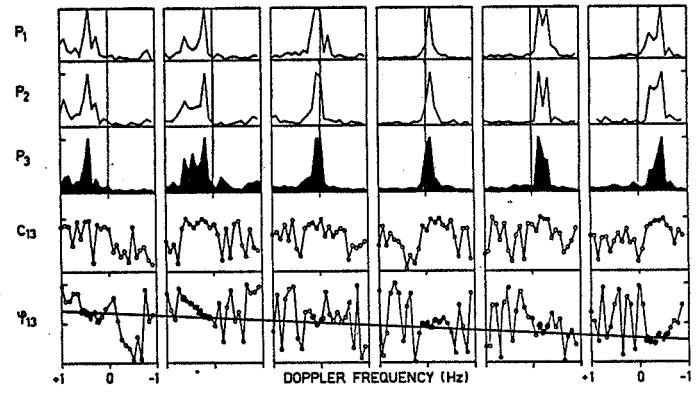

Figure 12. Power spectra P coherence C_{13} and phase ϕ_{13} of the mesospheric signal at z = 65 km. The straight line connects significant phase estimates at high coherence.

In summary we recognize that the application of the interferometer technique to MST/VHF radars is feasible and yields additional and very essential information on atmospheric structures and dynamics.

REFERENCES

Farley, D. T., H. M. Ierkic and B. G. Fejer (1981), Radar interferometry: A new technique for studying plasma turbulence in the ionosphere, J. Geophys. Res., 86, 1467-1472.

Kraus, J. D. (1966), Radio Astronomy, McGraw-Hill, New York.

Ierkic, H. M. and J. Rottger (1984), Mesospheric measurements of irregularity patches using a three-antenna interferometer, paper 3.6B, this volume.

Pfister, W. (1971), The wave-like nature of inhomogeneities in the E-region, J. Atmos. Terr. Phys., 33, 999-1025.

Rottger, H. and R. A. Vincent (1978), VHF radar studies of tropospheric velocities and irregularities using spaced antenna techniques, Geophys. Res. Lett., 5, 917-920.

Rottger, J. (1981), Wind variability in the stratosphere deduced from spaced antenna VHF radar measurements, Preprint volume 20th Conf. on Radar Meteorology, Boston, Am. Meteorol. Soc., 22-29.

Rottger, J. (1983), Techniques for measurements of horizontal and vertical velocities; Determination of horizontal and vertical wavelengths of gravity waves, Handbook for MAP, Vol. 9, 150-163; 262-267, SCOSTEP Secretariat, Dep. Elec. Computer Eng., Univ. IL, Urbana.

Rottger, J. (1984), The MST radar technique, Handbook for MAP, Vol. 13, 187-202, SCOSTEP Secretariat, Dep. Elec. Computer Eng., Univ. IL, Urbana.

Rottger, J., P. K. Rastogi and R. F. Woodman (1979), High-resolution VHF radar observations of turbulence structures in the mesosphere, Geophys. Res. Lett., 6, 617-620.

Royrvik, O. (1983), VHF radar signals scattered from the equatorial mesosphere, Radio Sci., 18, 1325-1335.

Vincent, R. A. and I. M. Reid (1983), HF Doppler measurements of mesospheric gravity wave momentum fluxes, J. Atmos. Sci., 40, 1321-1333.

Vincent, R. A. and J. Rottger (1980), Spaced antenna radar observations of tropospheric velocities and irregularities, Radio Sci., 15, 319-335.

Whitehead, J. D., W. R. From, K. L. Jones and P. E. Monro (1983), Measurements of movements in the ionosphere using radio reflections, J. Atmos. Terr. Phys., 45, 345-351.

Wohlleben, R. and H. Mattes (1973), Interferometrie in Radioastronomie und Radartechnik, Vogel-Verlag, Wurzburg.